Electronic Supplementary Information

Thiolated β-Cyclodextrin-based Host-Guest Interactions: Investigating and Tuning Chemical Interface Damping in Single Gold Nanorods

Minji Kim,[a] Yola Yolanda Alizar,[a] Rafifah Hana Raihana Syam,[a] and Ji Won Ha[a,*]

[a]Department of Chemistry, University of Ulsan, 93 Daehak-ro, Nam-gu, Ulsan 44610, Republic of Korea

*To whom correspondence should be addressed

J. W. Ha

Phone: +82-52-712-8012

Fax: +82-52-712-8002

E-mail: jwha77@ulsan.ac.kr

1. Experimental Methods

Materials and Chemicals.

β-Cyclodextrin (βCD; $C_{42}H_{70}O_{34}S$) was purchased from Ruixibiotech (China). Cholesterol (Cho; $C_{27}H_{46}O$, ≥99%), methyl orange (MO; $C_{14}H_{14}N_3NaO_3S$, 85 %), Sodium borohydride ($NaBH_4$, powder, ≥98.0%), Nafion ($C_7HF_{13}O_5S{\cdot}C_2F_4$, 0.5% solution) were purchased from Sigma-Aldrich. Hydrochloric acid (HCl, 35%), was purchased from DAEJUNG (South Korea). Cetyl trimethyl ammonium bromide (CTAB)-stabilized gold nanorods (AuNRs) was purchased from Nanopartz (Loveland, CO, USA).

Characterization of AuNRs. The ensemble extinction spectrum of AuNRs was obtained using a ultraviolet-visible (UV-Vis) spectrophotometer (UV-1800, SHIMADZU, Japan). The morphology and average size distribution of AuNRs were examined using a scanning electron microscope (SEM; JSM-6500F, JEOL, Japan).

Sample Preparation for Single Particle Spectroscopy. Slide glass (76 mm × 26 mm × 1 mm, MARIENFELD) and cover glass (22 mm × 22 mm, 24 mm × 50 mm, BRAND) were ultrasonically cleaned using ethanol, deionized (DI) water, and isopropyl alcohol for 15 min each. For sample preparation, an AuNR solution was diluted with DI water to achieve an approximate concentration of 1 μM AuNR, minimizing interparticle localized surface plasmon resonance (LSPR) coupling. The diluted AuNR solution was sonicated for 15 min at room temperature to prevent aggregation. The solution was then applied to a slide glass and allowed to dry. Next, an oxygen plasma cleaner (PDC-32G-2, Harrick Plasma, USA) was used to remove the CTAB layer surrounding the AuNRs. DI water was added as the surrounding

medium, and for dark-field (DF) microscopy-based scattering spectroscopy, a cover glass was placed on top of the slide glass.

Dark-Field Microscopy and Spectroscopy. To obtain the spectrum of single AuNR particles using a scattering-based DF microscope (ECLIPSE Ti-U, NIKON, Japan), we utilized an oil iris objective lens (NA 0.7–1.4) connected to an Andor CCD camera (Newton DU920P-OE, UK) coupled with an Andor spectrometer (SHAMROCK 303i, SR-303I-A). Light scattering from a single particle was collected by the objective lens and transmitted to the entrance of the spectrometer. The scattered light was dispersed through a grating (300-lines/mm) inside the spectrometer and detected by the CCD camera (central wavelength: 700 nm). Background spectra were measured in areas without nanoparticles. DF scattering images were obtained using an Andor EMCCD camera (iXon Ultra 897, UK). ImageJ software was used for image analysis, and data analysis was performed using MATLAB and Origin.

Sample Preparation for Raman Spectroscopy. For sample preparation, a 100 μL aliquot of the sample was transferred from the 1 mL AuNR stock solution to a centrifuge tube and centrifuged at 10,000 rpm for 10 min to remove the CTAB surfactant. The rinsed AuNR sample was resuspended in ethanol, and the probe-molecule solution was added to achieve the appropriate concentration. This colloidal solution was sonicated for 1 min to ensure adequate dispersion at room temperature. In real-time experiments, 1 mM of each reagent solution and AuNRs in ethanol were mixed using the sample prepared. After adding the probe-molecule solution to the rinsed AuNR solution, the prepared sample was immediately transferred to a capillary (diameter: 0.8–1.1 mm, wall thickness: 2.25 mm, length: 100 mm). Both ends of the capillary tube were sealed to prevent solvent evaporation.

Raman Spectroscopy. A custom-built Raman spectroscopic system with a 532-nm diode laser was used for all Raman and surface-enhanced Raman spectroscopy (SERS) measurements. A monochromator with a spectral resolution of 0.1 nm was equipped with a 600-lines/mm grating and a slit width of approximately 250 μm. The Raman spectra were collected using a 40× objective lens with a numerical aperture of 0.75. An Andor CCD camera (Newton DU920P-OE, UK) was used as the detector, while an Andor spectrometer (SHAMROCK 303i, SR-303I-A) transmitted the electronic data as spectra. All spectra were acquired and analyzed using MATLAB and Origin software.

Sample Preparation for Electrochemical Measurements. The glassy carbon electrode (GCE, 3 mm in diameter) was polished using sandpaper and alumina slurry, followed by cleaning with dilute nitric acid, ethanol, and distilled water successively in an ultrasonic bath. The cleaned electrode was then immersed in a 0.5 mol L^{-1} $[Fe(CN)_6]^{3-/4-}$ redox couple containing 0.1 M KCl, and the potential was cycled between -0.8V and 1.0 V until a steady-state potential was reached. For surface modification, 25 μL of AuNR@βCD was added to 1.0 mL of 0.5% Nafion solution, and the mixture was sonicated for 2 h to form a homogeneous mixture. Then, a 25 μL aliquot of the resulting suspension was drop-cast onto the prepared GCE surface and rinsed with ultrapure water. The electrode was subsequently incubated with 8.688 μM methylene orange (MO, 20 μL), rinsed with triple-distilled water, and air-dried at room temperature. After 1 min of deposition, the particle size and distribution on the surface became more uniform and homogeneous. The MO/βCD/AuNR/GCE electrode was then immersed in a 0.5 mol L^{-1} $[Fe(CN)_6]^{3-/4-}$ redox couple containing 0.1 M KCl for electrochemical measurement. Finally, the MO/βCD/AuNR/GCE electrode was rinsed with triple-distilled

water, and a fresh cholesterol (Cho, 25 μL) solution was incubated on the surface. After gentle washing with ultrapure water, the current response of the MO-conjugated Cho/βCD/GCE was measured using an electrochemical device.

Electrochemical Measurements. Electrochemical experiments were conducted using a three-electrode system with a custom-made electrochemical cell connected to a Multichannel Potentiostat (Metrohm Autolab/ M240-FRA32M). The system employed a GCE as the working electrode (WE), platinum (Pt) wires as the counter electrode (CE), and an Ag/AgCl reference electrode (RE). In this setup, the Ag/AgCl electrode served as the reference electrode. The experiments were carried out using a 0.5 mol L^{-1} $[Fe(CN)_6]^{3-/4-}$ redox couple with 0.1 M KCl as the supporting electrolyte.

2. Calculation of Surface Coverage of SH-βCD on AuNRs

We estimated the surface coverage of SH-βCD on AuNRs using a geometric approach. It is assumed that βCD molecules fully cover the AuNR surface and adopt a vertical orientation due to steric hindrance arising from their bulky size. The surface coverage can be calculated using the following equation (Eq. S1):

$$N_{\beta CD} = \frac{A_{AuNR}}{A_{\beta CD}} \qquad \text{Eq. S1}$$

Let A_{AuNR} represent the total surface area of a single AuNR (in nm²), and $A_{\beta\mathrm{CD}}$ the approximate footprint area of one βCD molecule on the surface (in nm²). The surface area of the AuNR is calculated using the formula for a cylinder with hemispherical caps:

$$\text{Surface area} = 2\pi rh + 4\pi r^2$$

Based on our measurements, the average dimensions of the AuNRs are 27.84(± 5.06) nm in diameter and 88.01(± 7.43) nm in length. From this, the calculated surface area of an AuNR is approximately 10,129.3 nm². For βCD, we assume a circular footprint based on its outer diameter of 1.54 nm, resulting in a footprint area of approximately 1.20 nm² (calculated using πr^2). Thus, we estimate the surface coverage of βCD on the AuNR to be approximately 1,570 molecules per AuNR under ideal full coverage conditions.

3. Statistical Analysis of LSPR Wavelength and Linewidth

We conducted the statistical analysis using one-way analysis of variance (ANOVA) to evaluate the differences in LSPR energy and FHWM shown in Figs. 5 and S11. Further encapsulation of MO into the βCD cavity led to an additional redshift ($p < 0.0001$) and linewidth broadening. However, the replacement of MO with Cho resulted in no significant change in the LSPR peak ($p = 0.82$) (Figs. 5C and S11) as both MO and Cho are encapsulated in βCD, the local dielectric environment around the nanoparticle surface is primarily influenced by the βCD host molecules. As a result, the LSPR peak position remains unchanged upon replacing MO with Cho, due to dielectric shielding in βCD. However, differences in guest molecule polarity, size, and charge transfer interactions are still expected to influence CID, which is reflected in the changes in linewidth rather than the LSPR peak.

The one-way ANOVA showed statistical difference between variants ($F=37.27$, $p < 0.0001$). To identify specific group differences, a Tukey HSD post-hoc analysis was conducted. Functionalization with βCD (AuNRs@βCD) and its MO complex (AuNRs@βCD/MO) significantly increased the FWHM compared to bare AuNR ($p<0.001$). Furthermore, the introduction of MO as a guest onto βCD (host) resulted in a significant increase in linewidth relative to AuNRs@βCD ($p=0.0013$). Interestingly, AuNRs@βCD/Cho showed a significantly lower FWHM than AuNRs@βCD/MO, suggesting a successful host-guest exchange. The differences in host-guest interactions influence the degree of linewidth broadening in AuNRs.

We further conducted the statistical analysis using one-way ANOVA to evaluate the differences in LSPR energy and FHWM shown in Fig. 6. One-way ANOVA revealed significant differences in LSPR [$F(2,258) = 44.86$, $p < 0.0001$] and FWHM [$F(2,258) = 93.51$, $p < 0.0001$], followed by Tukey's post hoc test. βCD/Cho adsorption caused a significant

redshift in LSPR ($p < 0.001$), while desorption induced a blueshift ($p < 0.001$) (Fig. 6B). FWHM increased after βCD/Cho adsorption ($p < 0.0042$), indicating enhanced CID, and decreased after $NaBH_4$-mediated thiol removal ($p = 0.023$) (Fig. 6C). $NaBH_4$ treatment shifted the LSPR peak back toward its original position and reduced FWHM, confirming effective desorption of βCD/Cho. These results demonstrate reversible tuning of CID and optical properties *via* controlled adsorption/desorption of thiolated βCD.

4. Supplementary Figures

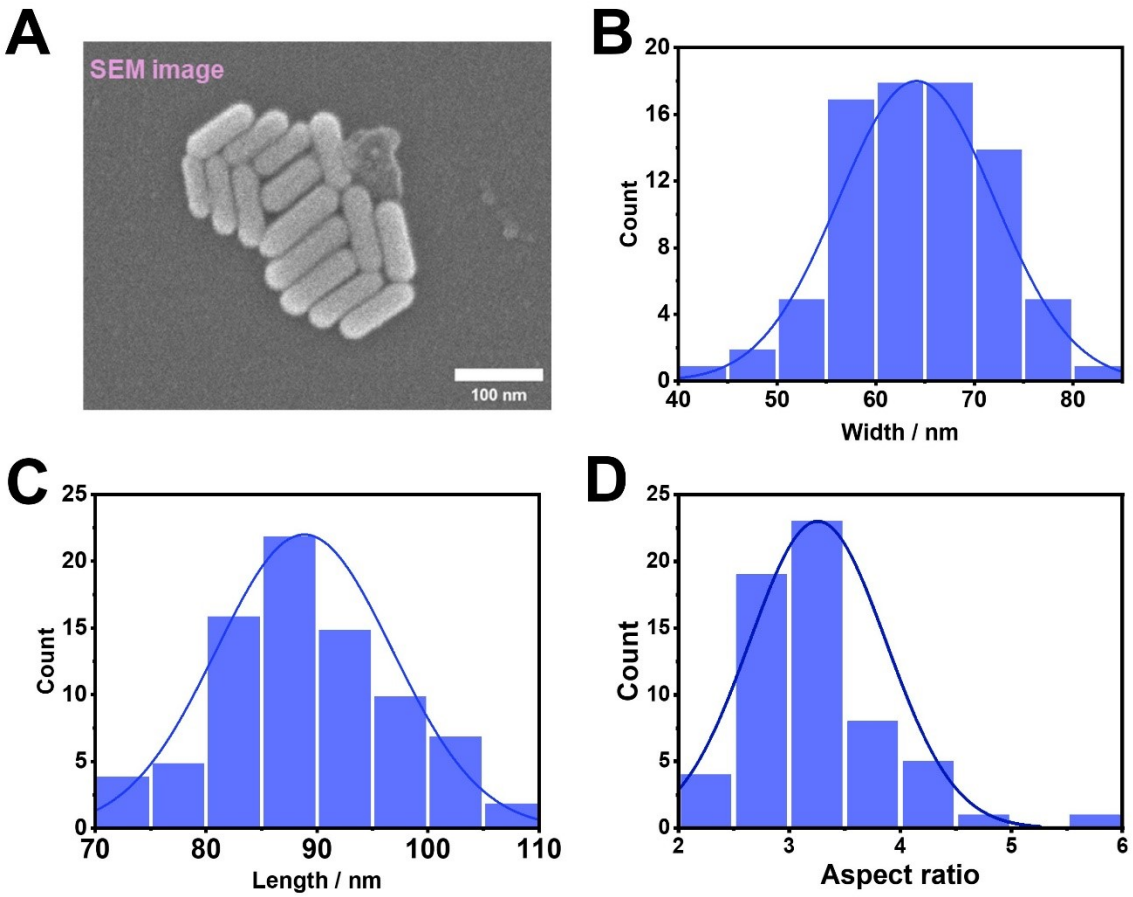

Fig. S1 (A) SEM image of bare AuNRs used in this study. Histograms showing the average **(B)** width, **(C)** length, and **(D)** aspect ratio of single AuNRs.

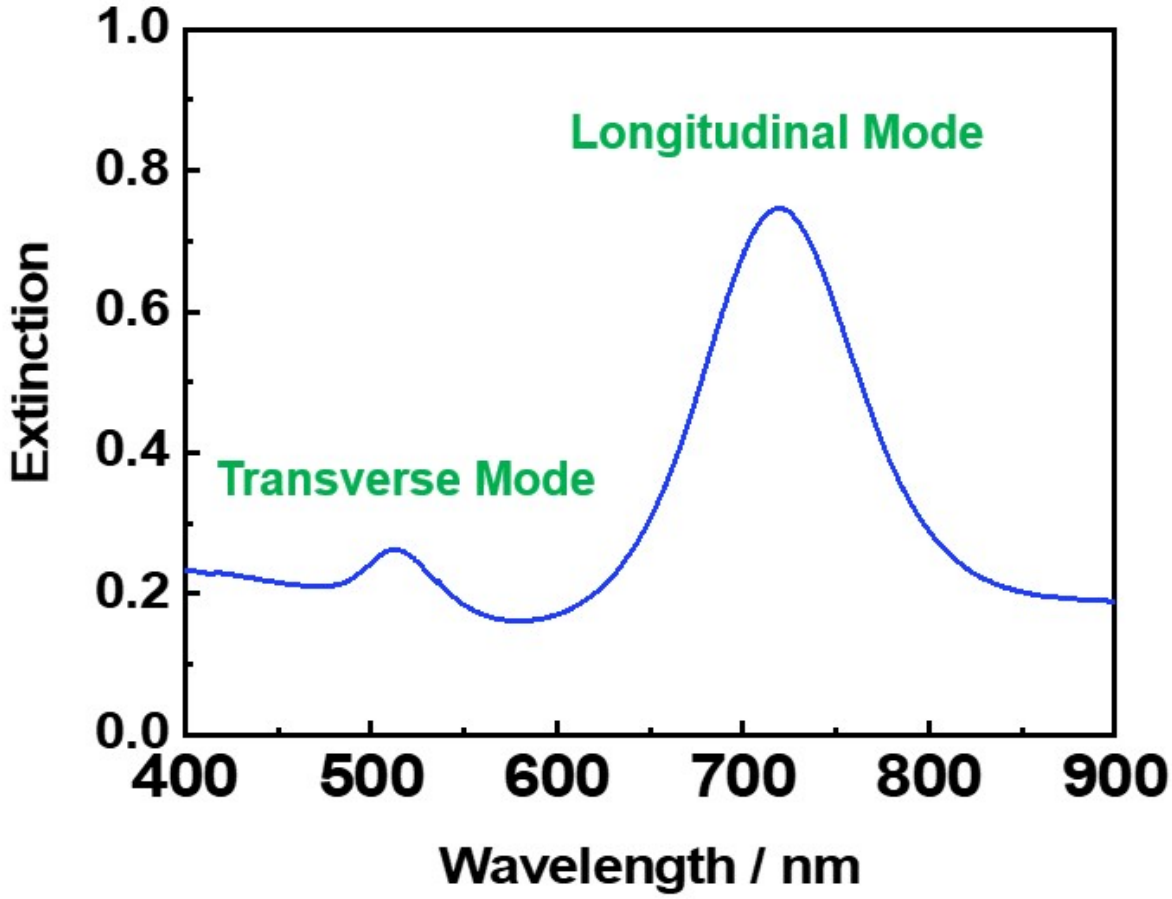

Fig. S2 The UV-Vis extinction spectrum of AuNRs dispersed in distilled water exhibited two LSPR peaks: a transverse peak at approximately 515 nm and a longitudinal peak at around 724 nm.

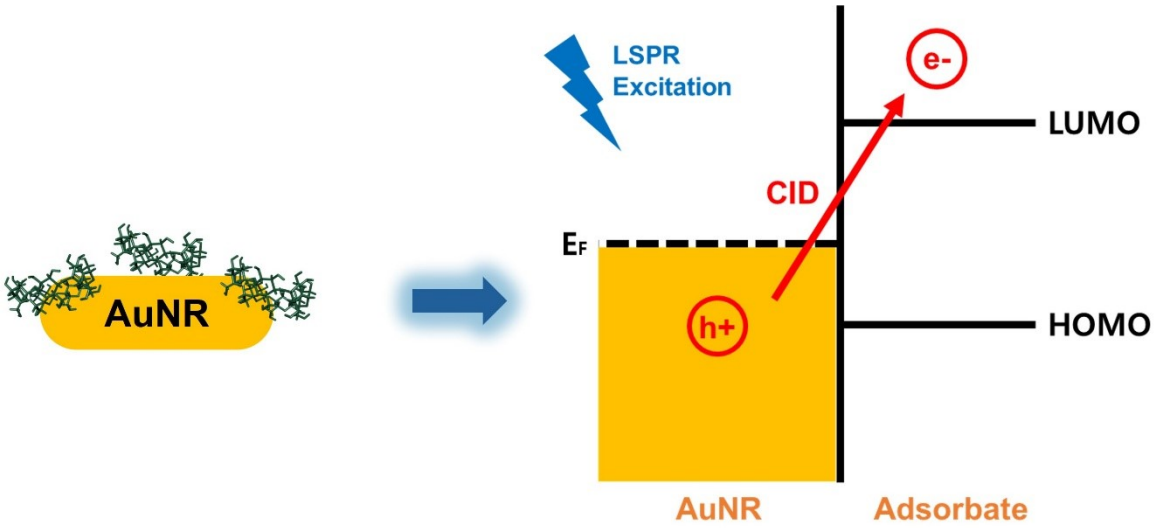

Fig. S3 Schematic diagram illustrating the thiolation of βCD on the AuNR surface, resulting in direct interfacial electron transfer from Au to the adsorbate (i.e., chemical interface damping, CID).

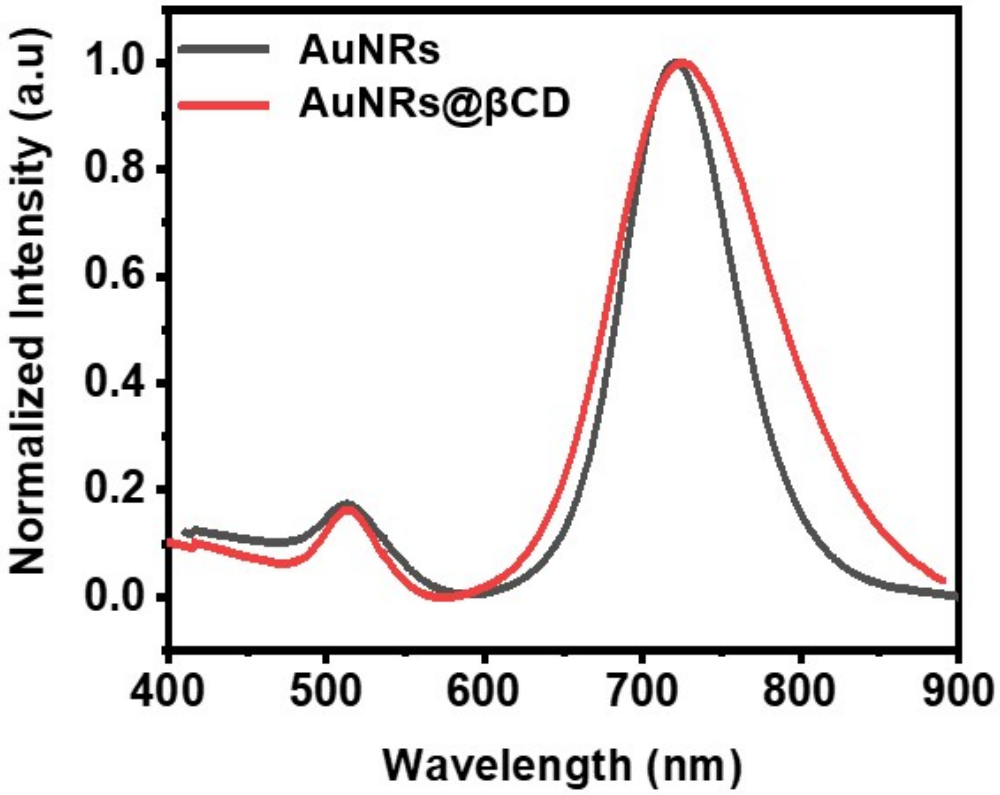

Fig. S4 UV-Vis extinction spectra to confirm the effective attachment of SH-βCD to AuNRs, which led to redshift and broadening of the LSPR peak after thiolation.

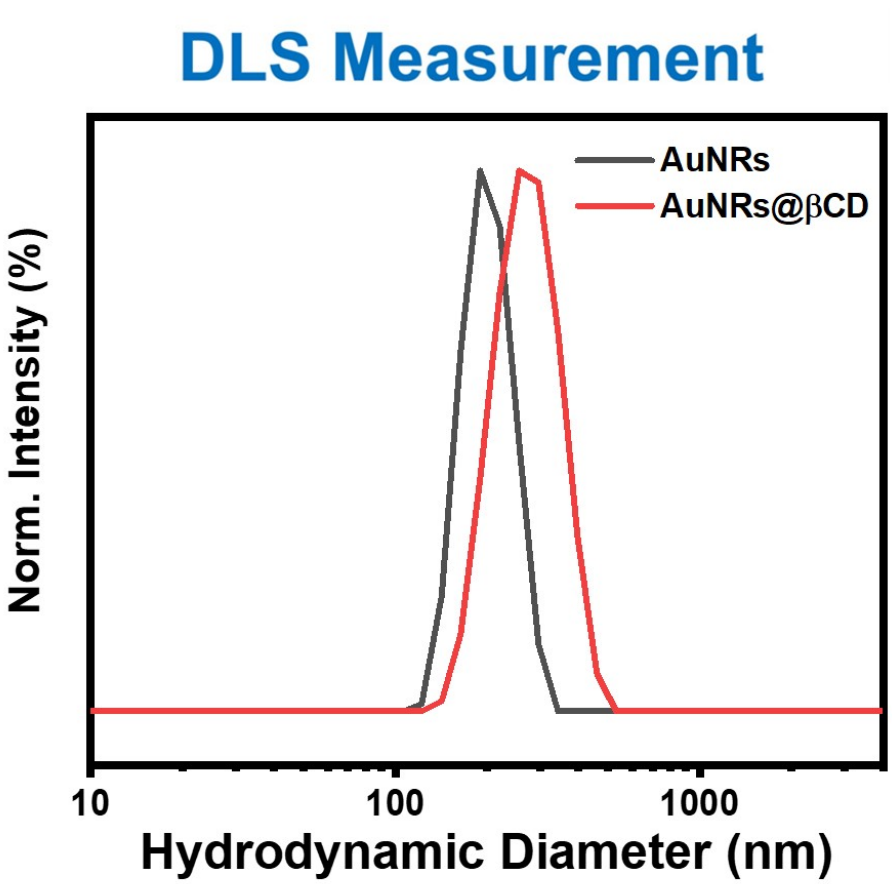

Fig. S5 Dynamic light scattering (DLS) measurement to confirm the effective attachment of SH-βCD to AuNRs.

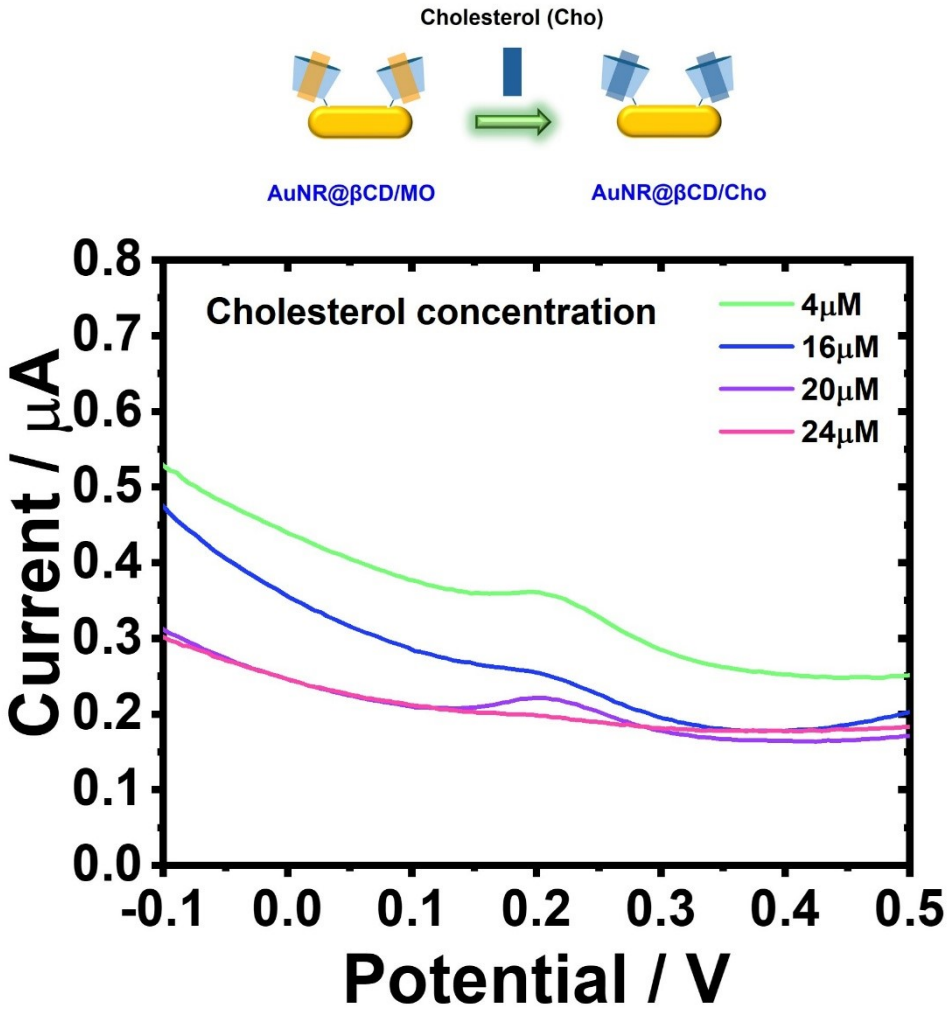

Fig. S6 Enlarged DPV curves of AuNR@βCD/MO in the presence of varying cholesterol concentrations, highlighted with a blue square in Fig. 3.

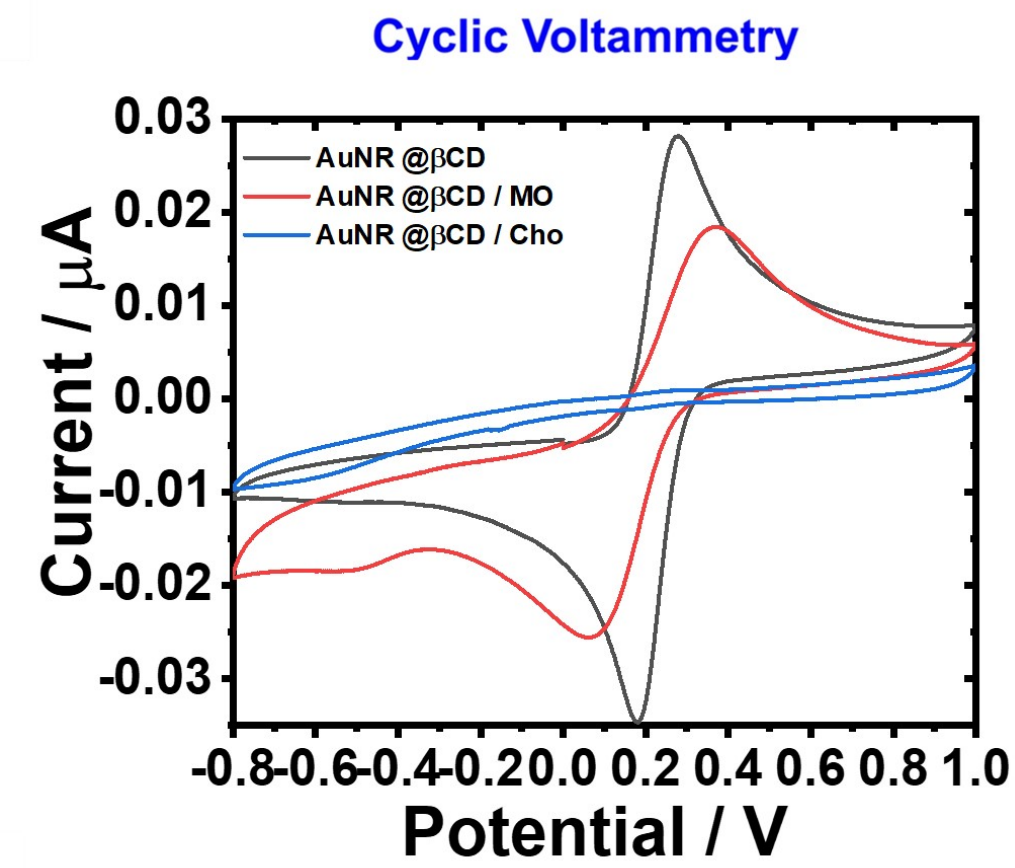

Fig. S7 CV curves of AuNR@βCD, AuNR@βCD/MO without Cho, and AuNR@βCD/MO after the addition of Chol, showing the replacement of MO by Cho.

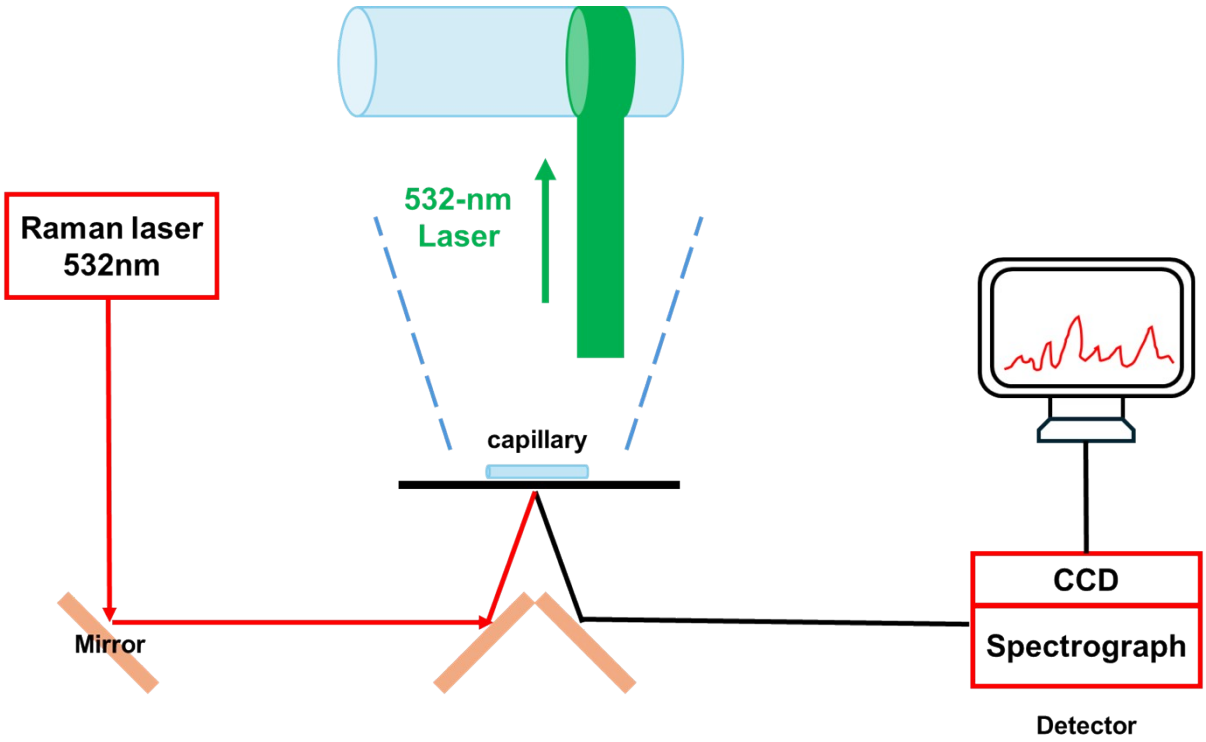

Fig. S8 Schematic illustrating the measurement process of AuNRs *via* Raman spectroscopy at 532 nm excitation.

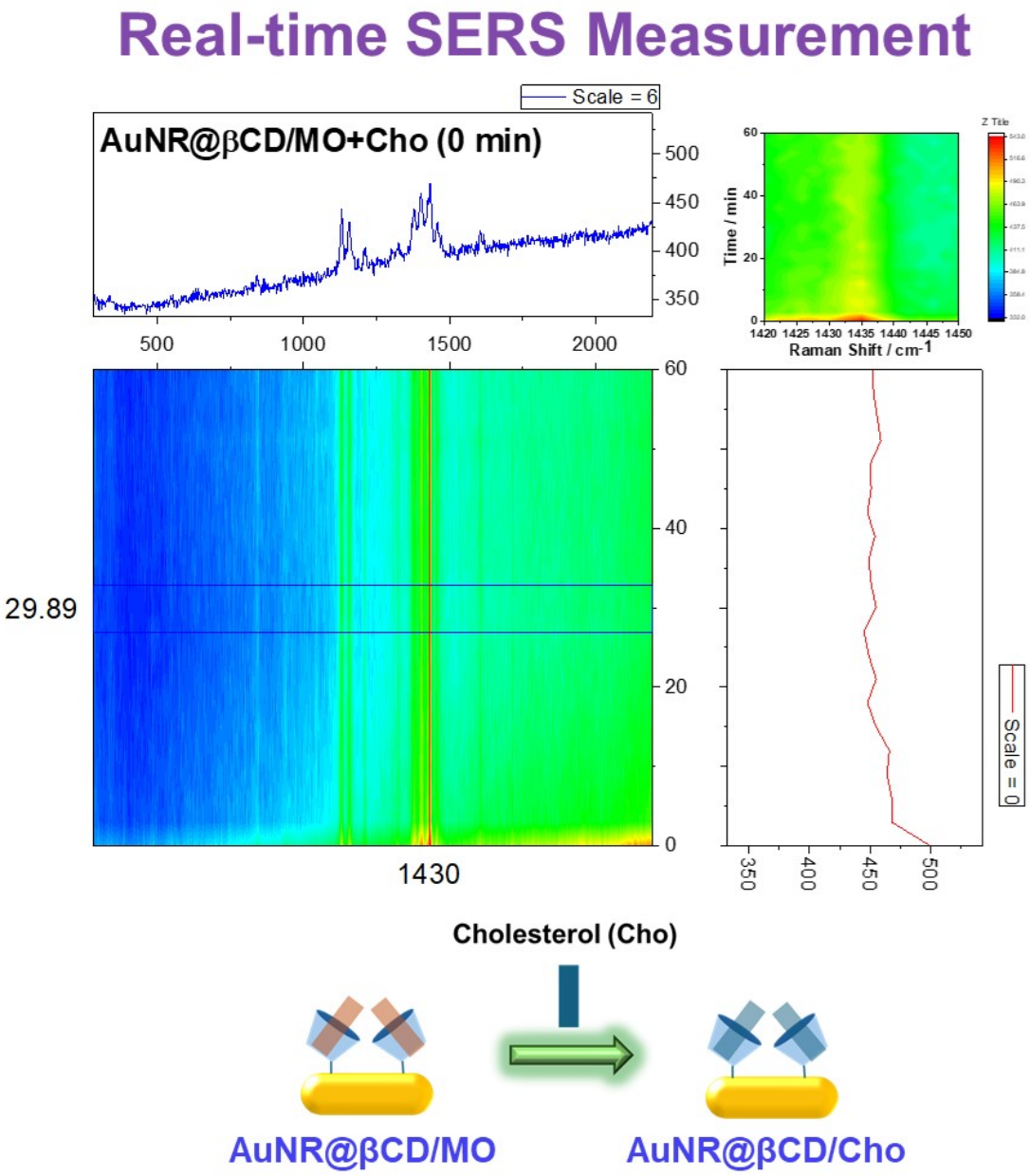

Fig. S9 Time-resolved SERS measurements of AuNR@βCD/MO after the addition of Cho. The intensity of the peak at 1430 cm^{-1}, corresponding to the C–C stretching vibration mode of MO, gradually decreased over time.

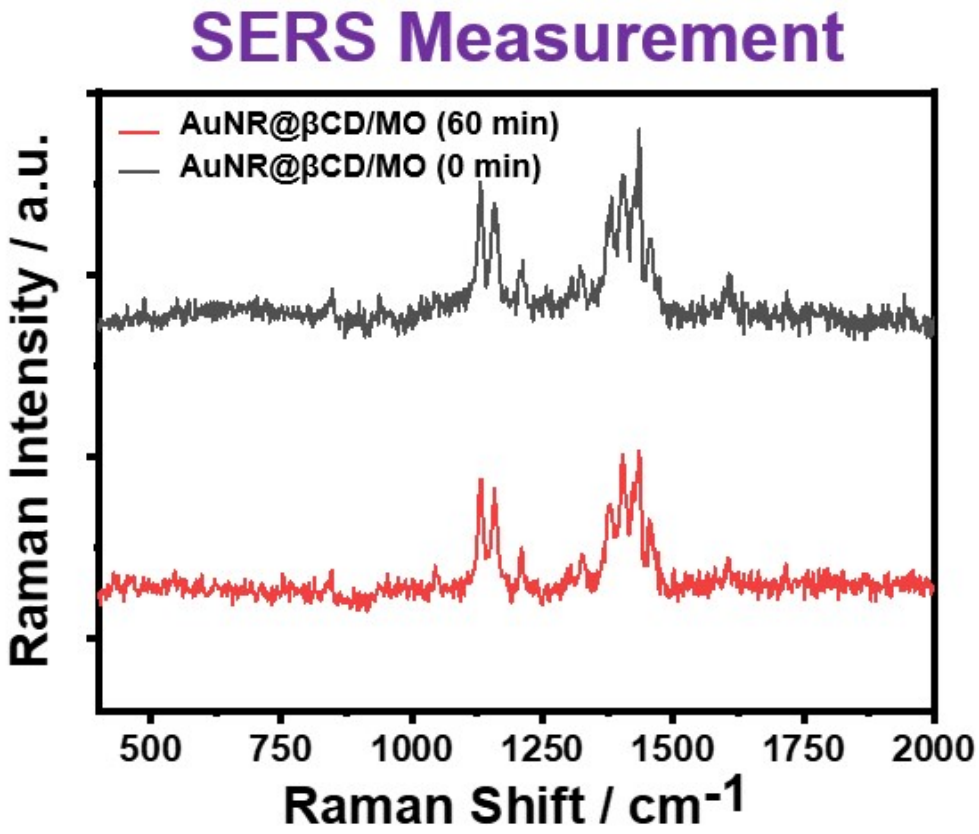

Fig. S10 Comparison of Raman spectra of AuNR@βCD/MO without adding Cho, recorded over 1 h, showing stable signals after 60 min.

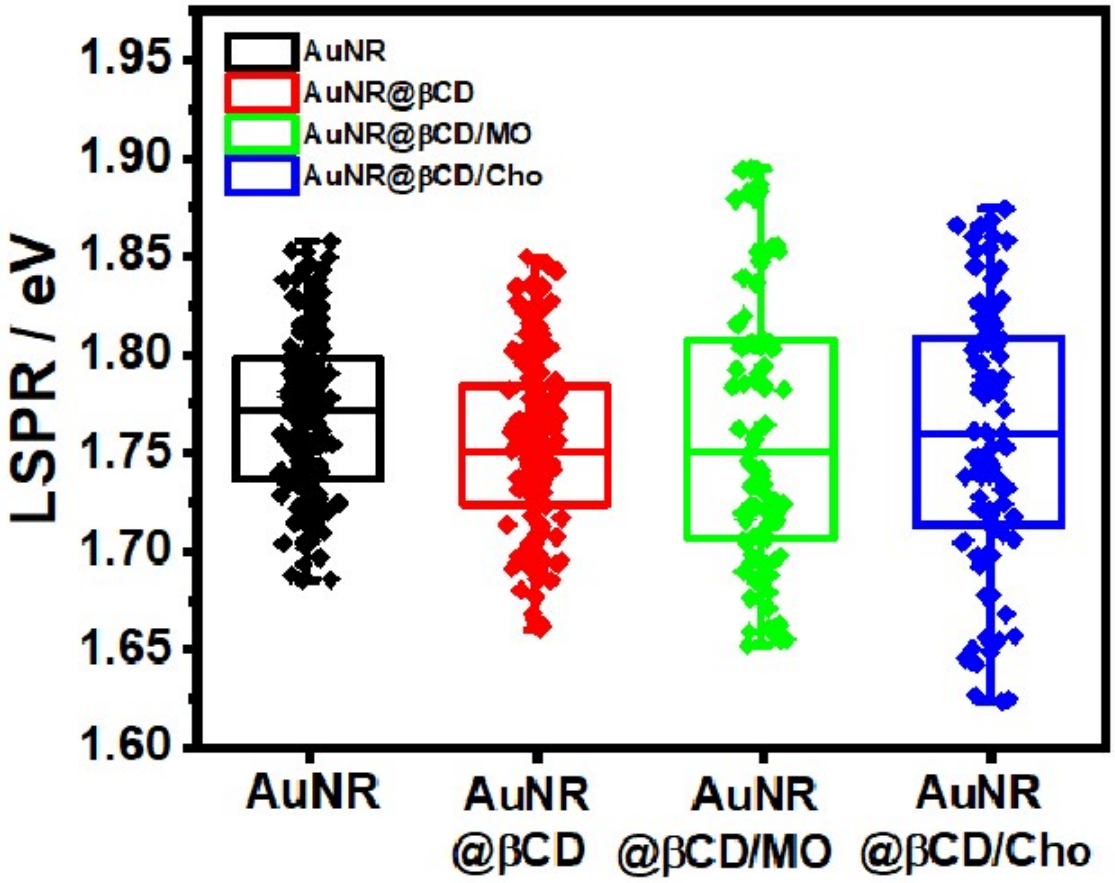

Fig. S11 Changes of LSPR wavelength of single AuNRs at each stage: bare AuNRs, AnRs@βCD, AuNRs@βCD/MO, and AuNRs@βCD/Cho.

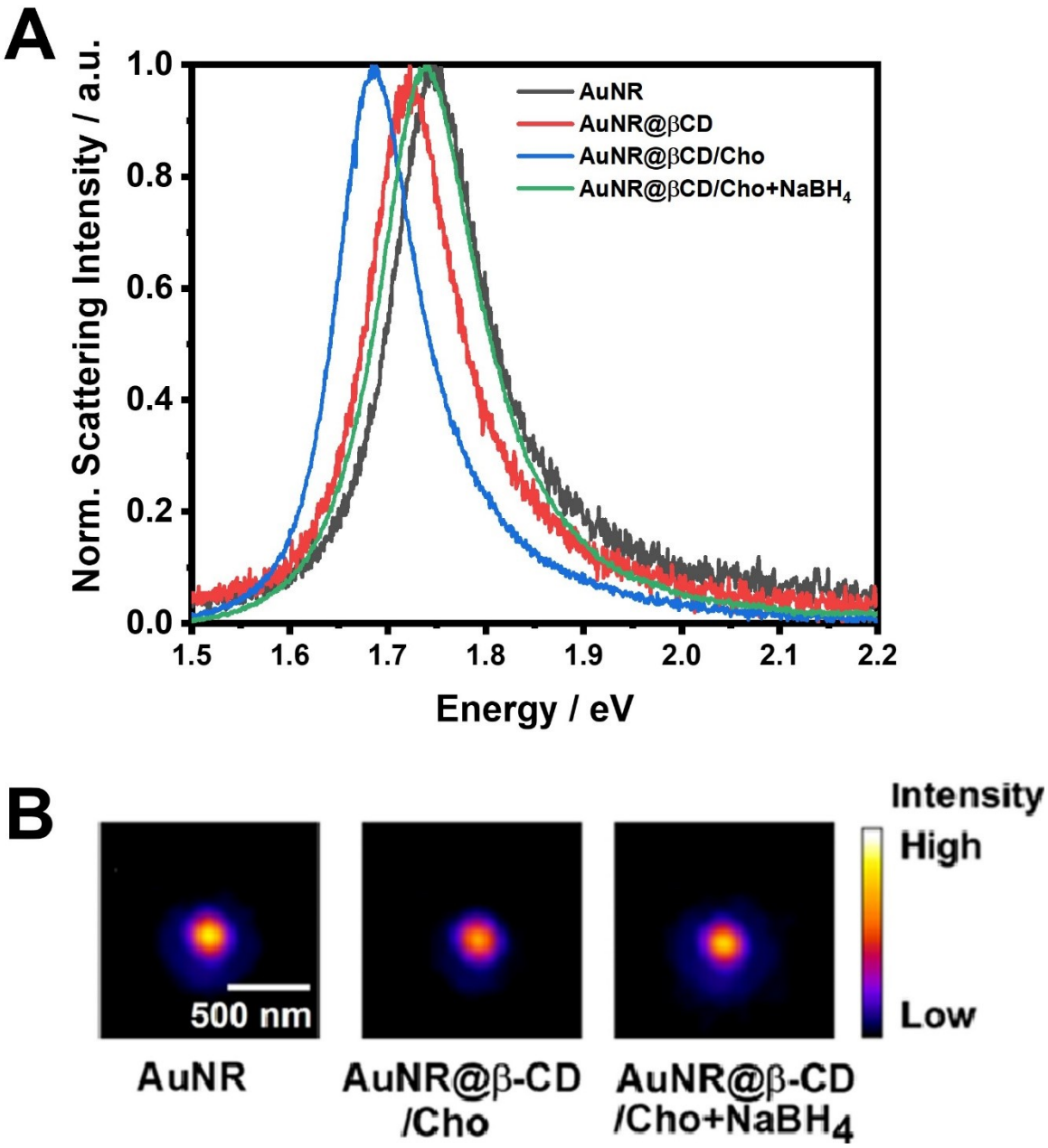

Fig. S12 (A) LSPR scattering spectra of a single AuNR recorded before and after adsorption of βCD and βCD/Cho, and again following $NaBH_4$ treatment at pH 12. **(B)** DF scattering images of the same single AuNR at each stage.

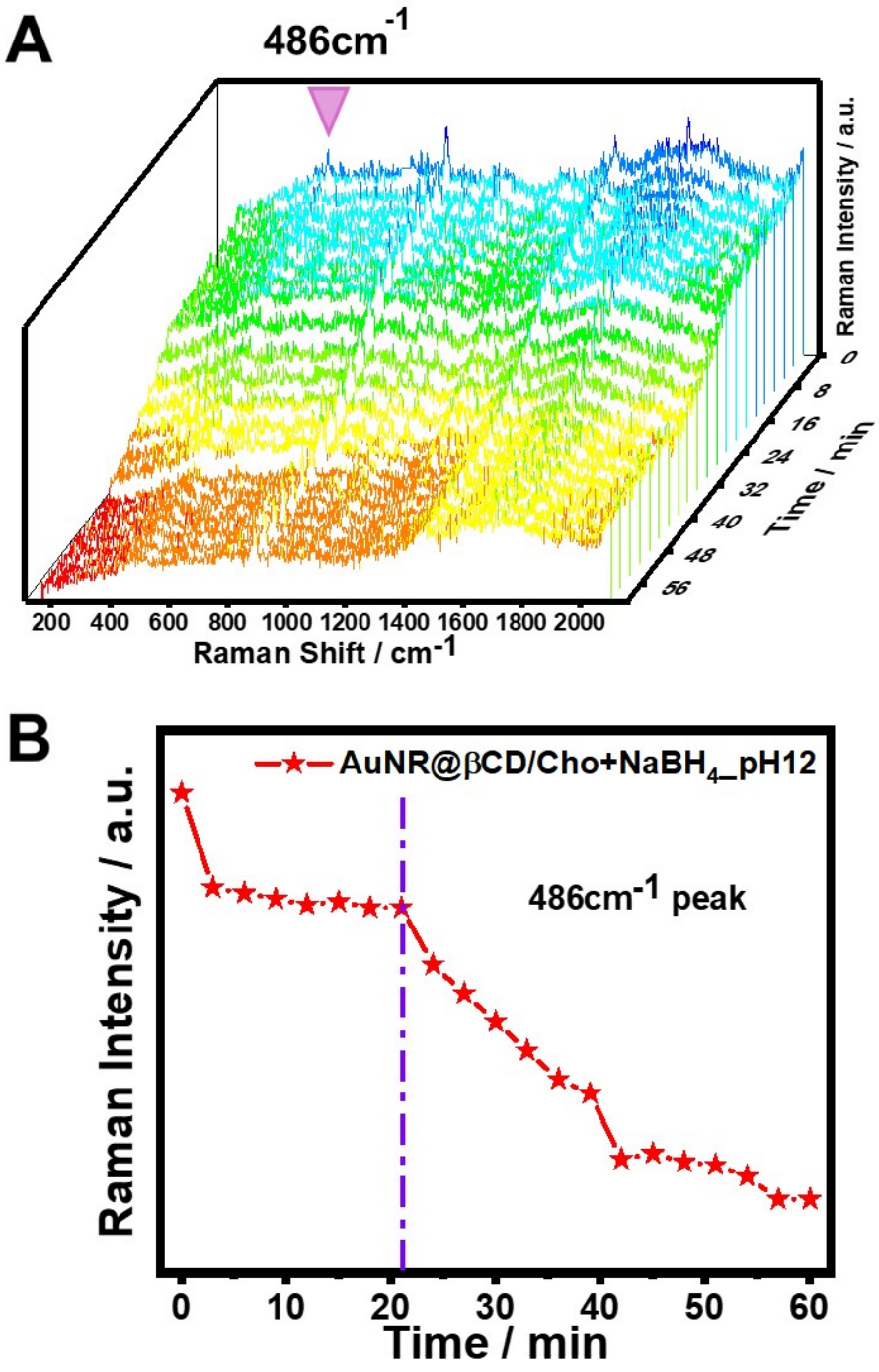

Fig. S13 $NaBH_4$-mediated thiol removal. **(A)** Real-time SERS spectra of AuNR@βCD/Cho in the presence of $NaBH_4$ at pH 12. **(B)** Time-dependent change in Raman intensity at 486 cm^{-1}, attributed to the C–H bending mode of Cho. A decrease in intensity over time is observed, indicating successful desorption of thiolated βCD/Cho from the AuNR surface.